# General description of quasi-adiabatic dynamical phenomena near exceptional points

Thomas J. Milburn,[1,*] Jörg Doppler,[2] Catherine A. Holmes,[3] Stefano Portolan,[4] Stefan Rotter,[2] and Peter Rabl[1]

[1] *Institute of Atomic and Subatomic Physics, Vienna University of Technology (TU Wien), Stadionallee 2, 1020 Vienna, Austria*
[2] *Institute for Theoretical Physics, Vienna University of Technology (TU Wien), 1040 Vienna, Austria*
[3] *University of Queensland, School of Mathematics and Physics, QLD 4072, Australia*
[4] *University of Southampton, Department of Physics and Astronomy, Southampton SO17 1BJ, United Kingdom*

The appearance of so-called exceptional points in the complex spectra of non-Hermitian systems is often associated with phenomena that contradict our physical intuition. One example of particular interest is the state-exchange process predicted for an adiabatic encircling of an exceptional point. In this work we analyse this and related processes for the generic system of two coupled oscillator modes with loss or gain. We identify a characteristic system evolution consisting of periods of quasi-stationarity interrupted by abrupt non-adiabatic transitions, and we present a qualitative and quantitative description of this switching behaviour by connecting the problem to the phenomenon of stability loss delay. This approach makes accurate predictions for the breakdown of the adiabatic theorem as well as the occurrence of chiral behavior observed previously in this context, and provides a general framework to model and understand quasi-adiabatic dynamical effects in non-Hermitian systems.

arXiv:1410.1882v3 [quant-ph] 23 Jun 2015

## I. INTRODUCTION

The quantum adiabatic theorem is a seminal result in the history of quantum mechanics. Paraphrasing Born, the theorem states that for an infinitely slow parametric perturbation there is no possibility of a quantum jump [1]. Many physical phenomena observed in both quantum and classical systems can be explained by this theorem, ranging from optical tapers [2] to robust quantum gates [3]. Recently, the applicability of adiabatic principles to non-Hermitian systems, e.g., coupled harmonic modes with gain or loss, has attracted considerable attention. Here, the complex eigenvalue structure and the existence of so-called exceptional points (EPs) leads to new counterintuitive phenomena [4–18]. Perhaps most strikingly, adiabatically encircling an EP was predicted to effect a state-exchange, with applications for switching and cooling [20–22]. However, it is now known that the very presence of non-Hermiticity prevents a general application of the adiabatic theorem [23–25], and the inevitability of non-adiabatic transitions leads to new effects, e.g., to chiral behavior [26–31].

Whereas the above results point to fascinating new physical phenomena, the complexity of the problem mostly requires one to resort to numerical studies (as cited above) or to focus on limiting cases where the system evolution is eventually dominated by a single mode with maximum gain or minimum loss. An important step beyond this limitation has recently been presented in Refs. [27] and [32] in which an exactly solvable model is considered and a connection between the appearance of non-adiabatic transitions and the Stokes phenomenon of asymptotics [33] is thereby found. However, even for very simple scenarios, these exact case studies are mathematically already quite involved, and the translation of the observed dynamics to other systems, in particular to realistic systems with imperfections and noise, is not immediately obvious.

In this work we analyse quasi-adiabatic dynamics in non-Hermitian systems near EPs with the aim to provide a generalised framework for both modelling and understanding the associated dynamical phenomena. Our approach reveals that the solutions are in general composed of periods of quasi-stationary during which the solution follows fixed points, interrupted by abrupt non-adiabatic transitions due to the exchange of stability. However, the time of these transitions cannot be predicted by a standard stability analysis, and, intriguingly, we find that piece-wise adiabaticity is still a key ingredient for understanding the evolution of the system in spite of an overall breakdown of adiabatic principles.

On a more fundamental level, our analysis shows that the quasi-adiabatic dynamics near an EP is a singularly perturbed problem [34], meaning that, in contrast to Hermitian systems, the dynamics cannot be obtained by perturbative corrections to the adiabatic prediction. This fact makes adiabatic principles in non-Hermitian systems particularly interesting as well as challenging to understand, both from a physical and from a mathematical point of view. Specifically, here we connect the problem of non-adiabatic transitions to the more general phenomenon of stability loss delay [35, 36] in dynamical bifurcations. This concept more easily affords intuition in complicated examples where exact solutions cannot be found and in realistic systems where noise cannot be ignored. Our results are therefore important for a variety of modern-day experiments with, e.g., waveguides [15, 16], coupled resonators [17, 18], semiconductor microcavities [19], or electromechanical [37, 38] and optomechanical systems [39–41], which offer sufficiently high control for the observation of the predicted dynamical phenomena.

* thomas.milburn@ati.ac.at

Typeset by REVTEX

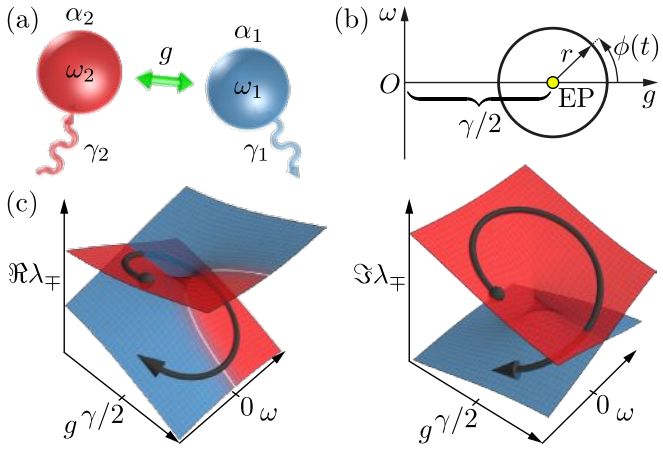


FIG. 1. (Color online.) (a) Cartoon of two coupled harmonic modes with gain or loss. (b) Example parametric path where $\gamma$ is fixed, $\omega = r\sin\phi(t)$, and $g = \gamma/2 + r\cos\phi(t)$. (c) Real ($\Re$) and imaginary ($\Im$) parts of the spectrum, $\lambda_\mp = \mp\sqrt{(\omega+i\gamma/2)^2+g^2}$. The curve is the trajectory of $\lambda_-$ for the path defined in (b) and depicts the fully adiabatic evolution.

## II. NON-HERMITIAN DYNAMICS AND EXCEPTIONAL POINTS

### A. Model

For the following discussion we consider the generic model of two coupled harmonic oscillators with frequencies $\omega_1$ and $\omega_2$, decay rates $\gamma_1$ and $\gamma_2$, and coupling strength $g$; see Fig. 1(a). The equations of motion for the amplitudes $\alpha_1$ and $\alpha_2$ are

$$\frac{d}{dt}\begin{pmatrix}\alpha_1\\ \alpha_2\end{pmatrix} = -i\begin{pmatrix}\omega_1 - i\gamma_1/2 & g\\ g & \omega_2 - i\gamma_2/2\end{pmatrix}\begin{pmatrix}\alpha_1\\ \alpha_2\end{pmatrix}, \quad (1)$$

where in general $\omega_i = \omega_i(t)$, $\gamma_i = \gamma_i(t)$, and $g = g(t)$ are functions of time. For the following analysis it is convenient to eliminate the common evolution with average frequency $\Omega := (\omega_2+\omega_1)/2$ and average decay rate $\Gamma := (\gamma_2+\gamma_1)/2$ by introducing a new set of amplitudes $\beta_1$ and $\beta_2$ via

$$\begin{pmatrix}\alpha_1(t)\\ \alpha_2(t)\end{pmatrix} = e^{-i\int^t[\Omega(t')-i\Gamma(t')/2]dt'}\begin{pmatrix}\beta_1(t)\\ \beta_2(t)\end{pmatrix}. \quad (2)$$

The remaining non-trivial dynamics in this frame is

$$\frac{d}{dt}\begin{pmatrix}\beta_1\\ \beta_2\end{pmatrix} = -i\begin{pmatrix}-\omega - i\gamma/2 & g\\ g & \omega + i\gamma/2\end{pmatrix}\begin{pmatrix}\beta_1\\ \beta_2\end{pmatrix}, \quad (3)$$

where $\omega := (\omega_2-\omega_1)/2$ and $\gamma := (\gamma_1-\gamma_2)/2$. Note that while the global transformation (2) does not affect any of the following results, if $\Gamma \neq 0$ then the experimentally observable amplitudes $\alpha_{1,2}$ are related to $\beta_{1,2}$ by an exponentially large or small prefactor.

Below we suppose that at least $\omega$ and $g$, or $\omega$ and $\gamma$ can be controlled as a function of time. This can be achieved, e.g., with optical modes propagating through waveguides with spatially varying losses [42, 43], by applying chirped laser pulses to molecular systems [28], or by using two mechanical resonators with electrically [37, 38] or optomechanically [39–41] controlled parameters.

### B. Exceptional points

Let us write Eq. (3) more compactly as $\dot{\vec{x}} = -i\mathbf{M}\vec{x}$, where $\vec{x}$ is the state vector and $\mathbf{M}$ is the dynamical matrix, or sometimes called in this context a non-Hermitian Hamiltonian [9], i.e.,

$$\vec{x} := \begin{pmatrix}\alpha_1\\ \alpha_2\end{pmatrix} \text{ and } \mathbf{M} := \begin{pmatrix}-\omega - i\gamma/2 & g\\ g & \omega + i\gamma/2\end{pmatrix}. \quad (4)$$

$\mathbf{M}$ has eigenvalues $\lambda_\mp = \mp\lambda = \mp\sqrt{(\omega+i\gamma/2)^2+g^2}$. The corresponding eigenvectors are

$$\vec{r}_- = \begin{pmatrix}\cos\vartheta/2\\ \sin\vartheta/2\end{pmatrix} \text{ and } \vec{r}_+ = \begin{pmatrix}-\sin\vartheta/2\\ \cos\vartheta/2\end{pmatrix} \quad (5)$$

with $\vartheta$ such that $\tan\vartheta = -g/(\omega+i\gamma/2)$. Figure 1(c) shows the real ($\Re$) and imaginary ($\Im$) parts of $\lambda_\pm$ as a function of $g$ and $\omega$ with $\gamma$ fixed. The pinch points $\omega + i\gamma/2 \mp ig = 0$ are EPs [4–10]. At these points the eigenvalues as well as the eigenvectors coalesce, and $\mathbf{M}$ becomes non-diagonalizable. Encircling an EP with a closed path in parameter space causes the two eigenvalues, and hence also the two eigenvectors, to swap; see Figs. 1(b, c). Based on intuition from the quantum adiabatic theorem, it was suggested that this unique feature could be observed in physical systems by encircling an EP over a time $T$ such that $T|\lambda_- - \lambda_+|$ is large [20–22]. However, other studies contradict this result and show that due to non-Hermiticity this picture cannot hold in general [23–31].

### C. Numerical examples

Before presenting a further analytic treatment of Eq. (3) we consider in Fig. 2 some typical solutions for encircling an EP with $T|\lambda_- - \lambda_+| \gg 1$. For these examples we choose a path in parameter space as defined in Fig. 1(b). We expand the solution as

$$\vec{x}(t) = c_-(t)\vec{r}_-(t) + c_+(t)\vec{r}_+(t), \quad (6)$$

where $\vec{r}_-(t)$ and $\vec{r}_+(t)$ are the *instantaneous* eigenvectors of $\mathbf{M}(t)$, and we choose the initial condition $c_-(0) = 1$ and $c_+(0) = 0$. The adiabatic prediction is $c_-^{\text{ad.}}(t) \simeq e^{-i\int_0^t \lambda_-(t')dt'}$ and $c_+^{\text{ad.}}(t) \ll c_-^{\text{ad.}}(t)$ [44–46].

In examples (i) and (ii) in Fig. 2 we have chosen an anticlockwise and a clockwise encircling respectively,

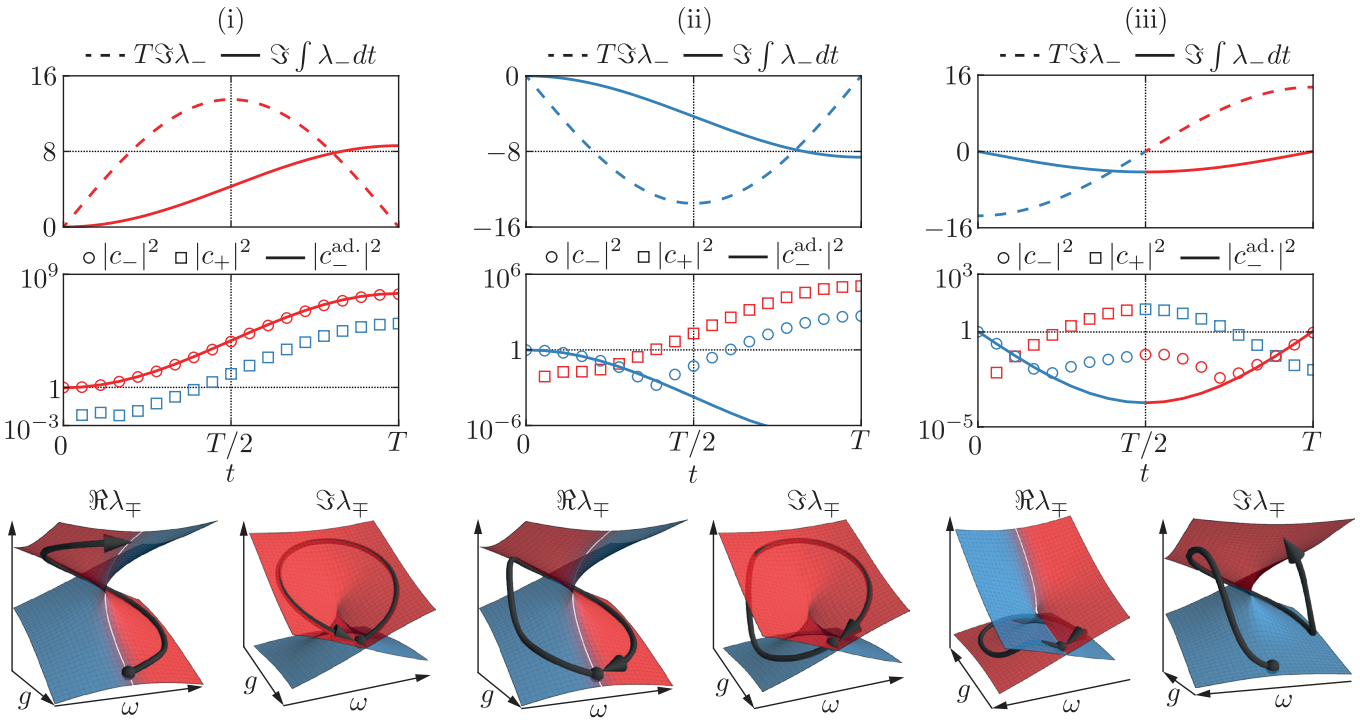


FIG. 2. (Color online.) Plots of typical numerical solutions of Eq. (3) for the path defined in Fig. 1(b) with initial eigenvector populations $c_-(0) = 1$ and $c_+(0) = 0$. For the function $\phi$ we choose $\phi(t) = \pm 2\pi t/T$ in examples (i, ii), and we choose $\phi(t) = -2\pi t/T + \pi$ in example (iii). In all cases we set $r = 0.1$, $\gamma = 1$ and $T = 45$, for which $T|\lambda_- - \lambda_+| \gg 1$. The top row shows the dynamical gain parameter, $T\Im\lambda_-(t)$, and the total integrated gain, $\int_0^t \Im\lambda_-(t')dt'$. Note that the dynamical gain is the gain of the adiabatic prediction but not necessarily the actual gain of the numerical solution. The middle row shows the eigenvector populations, $|c_\mp(t)|^2$, along with the adiabatic prediction, $|c_-^{\mathrm{ad.}}(t)|^2$. We do not plot $|c_+^{\mathrm{ad.}}(t)|^2$ because adiabatic principles imply $|c_+^{\mathrm{ad.}}(t)|^2 \ll |c_-^{\mathrm{ad.}}(t)|^2$. The bottom row shows a projection of the numerical solution onto the real and imaginary parts of the eigenspectrum, specifically $[|c_-(t)|^2\lambda_-(t) - |c_+(t)|^2\lambda_+(t)]/[|c_-(t)|^2 + |c_+(t)|^2]$. The use of red and blue is to provide an indication of which population, or surface, corresponds to a gain and loss eigenvector respectively.

$\phi(t) = \pm 2\pi t/T$. In the anticlockwise example the solution matches the adiabatic prediction and the corresponding state flips, but in the clockwise example we observe a non-adiabatic transition, for which, apart from an overall amplification, the system returns to the original state. This chiral behavior, first presented in Ref. [26], illustrates one of the key differences between the dynamics in Hermitian and non-Hermitian systems. In the latter, the eigenvalues are complex, which causes gain or loss in $c_-$ and $c_+$. An infinitesimally small non-adiabatic coupling can therefore be exponentially amplified, causing the gain eigenvector to dominate. This mechanism intuitively explains why the adiabatic theorem does not in general hold for non-Hermitian systems.

Example (iii) shows the result for a more interesting path $\phi(t) = -2\pi t/T + \pi$ where gain-loss behavior swaps half-way through and the total integrated dynamical gain vanishes, $\int_0^T \Im\lambda(t)dt = 0$. Surprisingly, the final state matches the adiabatic prediction, $|c_-(T)|^2 \simeq |c_-(0)|^2$, even though during the interim the solution is highly non-adiabatic. This observation cannot be explained by the intuitive argument above because $c_-$ is non-trivially slaved to $c_+$ past the time $t = T/2$ when we would expect $c_-$ to increase exponentially. Thus, considering dynamical gain alone is insufficient to accurately predict behaviour for quasi-adiabatic dynamics near EPs.

These basic examples illustrate that the dynamics of non-Hermitian systems involves three characteristic effects:

(i) The swapping of eigenvectors due to a $4\pi$-periodicity about an EP, which follows from the topology of the complex eigenvalue spectrum.

(ii) The appearance of enhanced non-adiabatic transitions due to the presence of gain or loss.

(iii) Periods of adiabatic evolution that persist significantly beyond the time of stability loss.

While (i) is readily incorporated by the eigenvector decomposition (6), we will now develop a general approach to describe the non-trivial interplay between (ii) and (iii).

## III. DYNAMICAL ANALYSIS

### A. Relative non-adiabatic transition amplitudes

In order to develop a general dynamical description we consider the evolution operator, $\mathcal{U}(t)$, defined by $\vec{x}(t) = \mathcal{U}(t)\vec{x}(0)$, which contains the full dynamics independent of the initial condition. In the eigenbasis Eq. (5), $\mathcal{U}(t)$ is the solution of

$$\dot{\mathcal{U}} = -i\begin{pmatrix} -\lambda(t) & -f(t) \\ f(t) & \lambda(t) \end{pmatrix}\mathcal{U}, \quad \mathcal{U} = \begin{pmatrix} \mathcal{U}_{-,-} & \mathcal{U}_{-,+} \\ \mathcal{U}_{+,-} & \mathcal{U}_{+,+} \end{pmatrix} \tag{7}$$

with initial condition $\mathcal{U}(0) = \mathbb{1}$, where

$$f(t) = \frac{g(t)\left[\dot{\omega}(t) + i\dot{\gamma}(t)/2\right] - \left[\omega(t) + i\gamma(t)/2\right]\dot{g}(t)}{2i\lambda^2(t)}, \tag{8}$$

is the non-adiabatic coupling [44]. Adiabaticity usually requires that the non-adiabatic coupling be much smaller than the distance between eigenvectors, $\varepsilon(t) := |f(t)/[2\lambda(t)]| \ll 1$. Since $\varepsilon(t) \propto T^{-1}$ this condition is always satisfied for an appropriate $T$. To set $f(t) = 0$ in Eq. (7), which would imply $\varepsilon(t) = 0$, would yield the diagonal adiabatic prediction

$$\mathcal{U}^{\text{ad.}}(t) = \begin{pmatrix} e^{-i\int_0^t \lambda(t')dt'} & 0 \\ 0 & e^{i\int_0^t \lambda(t')dt'} \end{pmatrix}. \tag{9}$$

However, as is evident in Fig. 2, even for arbitrarily small yet non-vanishing $\varepsilon(t)$ the actual solution is significantly non-diagonal. This indicates that the system is *singularly perturbed* by the non-adiabatic coupling, and $\mathcal{U}(t)$ cannot be obtained as a perturbative correction to $\mathcal{U}^{\text{ad.}}(t)$. We shall henceforth call $\varepsilon(t) \ll 1$ the *quasi*-adiabatic condition (see Appendix A 1 for more details).

In order to describe the non-adiabatic character of $\mathcal{U}(t)$ for quasi-adiabatic dynamics we focus on the relative non-adiabatic transition amplitudes [26]:

$$R_-(t) := \frac{\mathcal{U}_{+,-}(t)}{\mathcal{U}_{-,-}(t)} \text{ and } R_+(t) := \frac{\mathcal{U}_{-,+}(t)}{\mathcal{U}_{+,+}(t)}. \tag{10}$$

These describe the amount of non-adiabaticity in the solution. For example, $R_-(t)$ is a measure of the magnitude of the net non-adiabatic transition from $\vec{r}_-(t)$ to $\vec{r}_+(t)$. If $R_\mp(t) \ll 1$ then we may say that $c_\mp$ is behaving adiabatically, while $R_\mp(t) \gg 1$ indicates that a non-adiabatic transition has occurred. From Eqs. (7) and (10) it follows that $R_\mp(t)$ considered as a dynamical variable is the solution to the Riccati equation [32, 47]

$$\dot{R}_\mp = \mp 2i\lambda(t)R_\mp \mp if(t)(1 + R_\mp^2) \tag{11}$$

with initial condition $R_\mp(0) = 0$. Dynamical phenomena associated with quasi-adiabatically encircling EPs can thus be understood from the solutions of this equation in the limit $\varepsilon(t) \ll 1$. Note that the equations of motion for $R_-$ and $R_+$ are related via $R_- \leftrightarrow 1/R_+$. In the following, we therefore consider only $R := R_-$ without loss of generality.

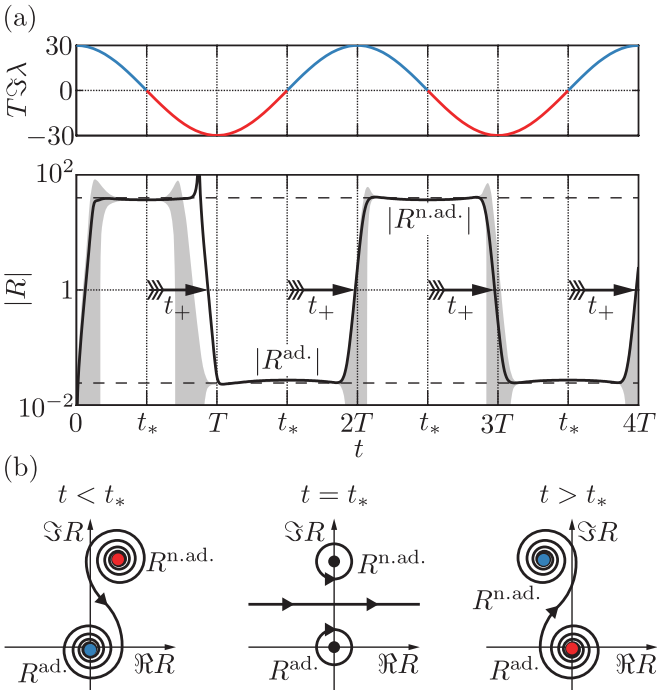


FIG. 3. (Color online.) (a) Plot of $\Im\lambda(t)$ (upper panel), and a typical solution for $R \equiv R_-$ (lower panel), for the path defined in Fig. 1(b) with $\phi(t) = -2\pi t/T + \pi$. Note that $\Im\lambda(t) = -\Im\lambda_-(t)$, which is plotted in Fig. 2. We have chosen $r = 0.1$, $\gamma = 1$ and $T = 100$, for which $\varepsilon(t) \simeq 2.5\%$. The solid curve is the numerical solution. The arrows denote delay times. The lower and upper dashed grid lines denote $|R^{\text{ad.}}(t)|$ and $|R^{\text{n.ad.}}(t)|$ respectively. The shaded area is one standard deviation about the mean of $R_-$ obtained from 10,000 stochastic numerical integrations of $c_-$ and $c_+$ (see Sec. IV for more details). (b) Cartoons of the global phase portraits of the equation of motion for $R$ near $t_*$. Arrows denote the direction of time-evolution along an integral curve. The fixed point near the origin corresponds to $R^{\text{ad.}}(t)$, and the fixed point far from the origin corresponds to $R^{\text{n.ad.}}(t)$.

We remark that, assuming transients are damped, the relation $R_- \leftrightarrow R_+$ has the immediate consequence that $\lim_{t\to\infty} R_-(t)R_+(t) = 1$, which agrees with Ref. [26] and prohibits simultaneous adiabatic behaviour in both $c_-$ and $c_+$ over long times.

### B. Fixed points and stability loss delay

The lower panel of Fig. 3(a) shows a generic solution for $R$ during multiple quasi-adiabatic encirclements of an EP (see the caption for details). It resembles a square wave, i.e., we see fast switching between two quasi-stationary values. This behavior can be understood from a separation of time-scales in Eq. (11). For short times the

slowly varying parameters $\lambda(t) \simeq \lambda$ and $f(t) \simeq f$ can be considered constant and

$$\dot{R} \simeq -2i\lambda R - if(1+R^2). \tag{12}$$

On a fast time-scale set by $|\Im\lambda|^{-1}$ the solution therefore approaches one of two fixed points

$$\begin{aligned} R^{\text{ad.}} &= -\frac{\lambda}{f}\left(1-\frac{\sqrt{\lambda^2-f^2}}{\lambda}\right) \simeq -\frac{f}{2\lambda} \text{ and} \\ R^{\text{n.ad.}} &= -\frac{\lambda}{f}\left(1+\frac{\sqrt{\lambda^2-f^2}}{\lambda}\right) \simeq -\frac{2\lambda}{f}. \end{aligned} \tag{13}$$

The first fixed point, $R^{\text{ad.}}(t) \propto \varepsilon(t) \ll 1$, indicates adiabatic behavior ($c_-$ dominates) and is stable for $\Im\lambda(t) < 0$. The second fixed point, $R^{\text{n.ad.}}(t) \propto \varepsilon^{-1}(t) \gg 1$, indicates a non-adiabatic transition has occured ($c_+$ dominates) and is stable for $\Im\lambda(t) > 0$. These two fixed points are plotted in Fig. 3(a). Evidently, the periods of quasi-stationarity there exhibited correspond to following one of these two fixed points.

On a slow time-scale set by $T$ the parameters $\lambda(t)$ and $f(t)$ may change considerably and at certain critical times the stability of the two fixed points swaps. For example, $R^{\text{ad.}}(t)$ becomes unstable and $R^{\text{n.ad.}}(t)$ stable when the sign of $\Im\lambda(t)$ becomes positive. Let us denote the critical times by $t_*$, which are marked in Fig. 3(a). Naïvely, one might expect an immediate rapid transition between the neighbourhoods of $R^{\text{ad.}}(t)$ and $R^{\text{n.ad.}}(t)$ upon passing a critical time $t_*$, but, as is evident in Fig. 3(a), this is not the case. Instead, we see that the solution follows, e.g., $R^{\text{ad.}}(t)$ while it is unstable for a significant amount of time; the loss in stability is delayed. Intuition for this behaviour is obtained from the phase portraits of Eq. (11), shown in Fig. 3(b). The local phase portrait about $R^{\text{ad.}}(t)$ goes from a spiral towards $R^{\text{ad.}}(t)$ for $t < t_*$ to a spiral away from $R^{\text{ad.}}(t)$ for $t > t_*$, passing through a degenerate bifurcation at $t = t_*$ when $R^{\text{ad.}}(t)$ is a centre and neither stable nor unstable. We therefore expect some persistence in the following of $R^{\text{ad.}}(t)$ because near $t_*$ it is only 'weakly' stable or unstable.

To illustrate the existence of a significant delay between the critical time $t_*$ and the actual time of a non-adiabatic transition $t_+$ we consider the specific path defined in Fig. 1(b) with $\phi(t) = -2\pi t/T + \pi$ and $r \ll \gamma$. This is a good model for the numerical solution shown in Fig. 3(a). Then, $\lambda(t) \simeq i\sqrt{r\gamma}e^{-i\pi t/T}$, $f(t) \simeq i\pi/(2\,T)$, and $\varepsilon(t) \simeq \varepsilon = \pi/(4\sqrt{r\gamma}\,T)$. Let us focus on the loss of stability of $R^{\text{ad.}}(t)$ at $t_* = 3T/2$. Assuming that the system is near $R^{\text{ad.}}(t)$ we can neglect the nonlinear term in Eq. (11):

$$\frac{\dot{R}}{2\sqrt{r\gamma}} \simeq e^{-i\pi t/T}R + \varepsilon. \tag{14}$$

The particular integral of this equation is found to be

$$R(t) = -\frac{i}{2}E_1\left(\frac{i}{2\varepsilon}e^{-i\pi t/T}\right)e^{i\exp(-i\pi t/T)/(2\varepsilon)}, \tag{15}$$

where $E_1$ is the exponential integral. Since $\varepsilon \ll 1$ we may use the asymptotic expansion for $E_1$ (see, e.g., 5.1.7 and 5.1.51 in Ref. [48]) to obtain

$$\begin{aligned} R(t) \simeq\ & -\varepsilon e^{i\pi t/T} - 2i\varepsilon^2 e^{2i\pi t/T} + \dots \\ & - \frac{\pi}{2}\,\text{sgn}\left[\cos\left(\frac{\pi t}{T}\right)\right]e^{i\exp(-i\pi t/T)/(2\varepsilon)}. \end{aligned} \tag{16}$$

The first two terms (upper line on the right) correspond to following $R^{\text{ad.}}(t)$ with higher order corrections. The third term (lower line) is negligible for $(t - t_*) < T/2$ (recall $t_* = 3T/2$ here), but it diverges exponentially for $(t - t_*) > T/2$, thereby indicating a non-adiabatic transition. Thus, under the ideal conditions assumed here and given that the solution has approached $R^{\text{ad.}}(t)$ by $t = t_*$, the delay in the loss of stability is $(t_+ - t_*) = T/2$.

With this analysis we are already in a position to understand better the three examples studied in Fig. 2. In example (i) $R^{\text{ad.}}(t)$ is stable for the entire loop around the EP and therefore the solution follows the adiabatic prediction, $|c_+(t)/c_-(t)| \simeq |R^{\text{ad.}}(t)|$. In contrast, in (ii) $R^{\text{ad.}}(t)$ is always unstable and a non-adiabatic transition occurs. In (iii) the solution first switches from $R^{\text{ad.}}(t)$ to $R^{\text{n.ad.}}(t)$, but then back again with a delay $t_+ \lesssim T/2$ after $R^{\text{ad.}}(t)$ becomes stable at $t = T/2$. Note that the delay times exhibited in the first encircling period as seen in Figs. 2 and 3(a) differ somewhat from the value $t_+ = T/2$ estimated above. This is due to a high sensitivity to the initial condition $R(0) = 0$, which is not exponentially close to $R^{\text{ad.}}(0)$, and therefore effects a transient term of the form $Ae^{i\exp(-i\pi t/T)/(2\varepsilon)}$. After about one encircling period the system approaches the unique long-time relaxation oscillation which is a universal signature of quasi-adiabatically encircling EPs.

We finish this section with a remark on the relation between the above results and the *Stokes phenomenon of asymptotics*, i.e., the switching-on of exponentially suppressed terms in asymptotic expansions [33]. In Refs. [27, 32] an exact solution for the example considered in this subsection is presented (using $r \ll \gamma$ but not neglecting the nonlinearity), which we review in Appendix B. In this exact solution one sees that the sharp (but continuous) transition, which in Eq. (16) is represented by the signum function, is precisely the Stokes phenomenon of asymptotics, leading here to a breakdown of the adiabatic theorem. In our current approach, which we elaborate further in the next section, this discontinuity is connected to the problem of stability loss delay. To our knowledge the connection between the Stokes phenomenon of asymptotics and stability loss delay has hitherto not been suggested, and might be worth exploring further. However, here we will leave such considerations aside and proceed with a pragmatic generalisation of these initial results to arbitrary paths in parameter space.

### C. Generalised quasi-adiabatic solution

In the previous section, Sec. III B, we were able to understand the generic solution exhibited in Fig. 3(a) from a separation of time-scales, which resulted in a delay in the loss of stability of the instantaneous fixed points. In fact, slow-fast systems with dynamical bifurcations are a subject of current mathematical interest. The reader is referred to Ref. [34] for a concise description. The reason that the critical times do not coincide with the observed times when an instantaneous fixed point loses stability is because our slow-fast system is *singularly perturbed*; the slow system is described by an algebraic equation, while the fast system by a differential equation. One must therefore resort to non-standard analysis. A principal result of the non-standard analysis of slow-fast systems is the existence of *stability loss delay* about certain dynamical bifurcations [35, 36, 49], which we observed explicitly in Sec. III B. In the following we build upon this to construct a generalised quasi-adiabatic solution, which, additionally, affords an estimation of delay times.

We are interested in solutions that for times near critical times $t_*$ are in the vicinity of a fixed point. We therefore begin by looking at the zero-crossings of $\Im\lambda(t)$, which determine $t_*$. For some window $[t_-, t_+]$ about each $t_*$, i.e., $t_- < t_* < t_+$, we seek a solution $R_{t_*}(t)$ that follows $R^{\text{ad.}}(t)$ or $R^{\text{n.ad.}}(t)$. Since transitions between $R^{\text{ad.}}(t)$ and $R^{\text{n.ad.}}(t)$ are very quick, by making a piece-wise addition of segments that follow one or the other fixed point we arrive at the approximation for the complete solution thus

$$R(t) \simeq \sum_{t_*} [\Theta(t-t_-) - \Theta(t-t_+)] R_{t_*}(t), \tag{17}$$

where $\Theta$ is the Heaviside step function.

Let us now consider a single segment and omit the subscript $t_*$ for brevity. We may focus on the case that $R(t)$ follows $R^{\text{ad.}}(t)$ without loss of generality because $R^{\text{n.ad.}}(t) = 1/R^{\text{ad.}}(t)$ and Eq. (11) is antisymmetric under the transformation $R \mapsto 1/R$. Since we assume $R(t)$ to be in the vicinity of $R^{\text{ad.}}(t)$ for $t \in [t_-, t_+]$ we study the linearised equation of motion about $R^{\text{ad.}}(t)$:

$$\dot{R} = -2i\lambda(t)R - if(t). \tag{18}$$

The general solution from time $t = t_0$ of this equation is

$$R(t) = R(t_0)e^{\Psi(t)-\Psi(t_0)} - i\int_{t_0}^{t} dt' f(t') e^{\Psi(t)-\Psi(t')}, \tag{19}$$

where $R(t_0)$ is the initial condition and

$$\Psi(t) = -2i\int_{t_*}^{t} \lambda(t')dt'. \tag{20}$$

Note that, to first order about $t_*$ we have $\lambda(t) = \lambda(t_*) + \dot{\lambda}(t_*)(t-t_*) + \mathcal{O}((t-t_*)^2)$. Since $\Im\lambda(t_*) = 0$ and $\Im\dot{\lambda}(t_*) > 0$ then $\Re\Psi(t) = \Im\dot{\lambda}(t_*)(t-t_*)^2 + \mathcal{O}((t-t_*)^3)$ is convex. We refer to this property of $\Psi$ below. Integrating the integral in Eq. (19) by parts $N$ times yields

$$\begin{aligned} R(t) =& [R(t_0) - \mathcal{R}^{\text{ad.}}(t_0)] e^{\Psi(t)-\Psi(t_0)} \\ &+ \mathcal{R}^{\text{ad.}}(t) + \Delta(t) e^{\Psi(t)}. \end{aligned} \tag{21}$$

Here we have introduced

$$\mathcal{R}^{\text{ad.}}(t) = \sum_{n=0}^{N-1} \left(\frac{-1}{2i\lambda(t)}\frac{d}{dt}\right)^n R^{\text{ad.}}(t), \tag{22}$$

which encapsulates the following of $R^{\text{ad.}}(t)$: The $n = 0$ term in $\mathcal{R}^{\text{ad.}}(t)$ is simply $R^{\text{ad.}}(t)$, and the higher order terms are corrections due to finite variations in $\lambda(t)$ and $f(t)$. However, since each term in the sum contains a derivative and therefore scales with $n!$, there is an optimal truncation $N = N_{\text{op.}}$ beyond which the sum diverges. The precise value of $N_{\text{op.}}$ is problem-specific, but for most purposes including only the first few terms in the sum Eq. (22) is sufficient.

The final term in Eq. (21), $\Delta(t)e^{\Psi(t)}$, is the remaining part of the solution which is not included in the sum Eq. (22). It therefore describes the non-trivial part of the dynamics that inevitably causes a departure from $R^{\text{ad.}}(t)$. Since $\Delta(t)e^{\Psi(t)}$ is the remainder of an optimally truncated sum it is negligible whenever the solution follows $R^{\text{ad.}}(t)$. On the other hand, for times $t \approx t_+$ when $\Delta(t)e^{\Psi(t)}$ starts to dominate, $\mathcal{R}^{\text{ad.}}(t)$ is negligible and we may approximate

$$\Delta(t)e^{\Psi(t)} \simeq -ie^{\Psi(t)}\int_{t_0}^{t} dt' f(t') e^{-\Psi(t')}. \tag{23}$$

Since $\Re\Psi$ is convex and since $\Psi(t) \propto \varepsilon^{-1}(t)$, the integrand in Eq. (23) is non-negligible only for times $t' \approx t_*$ and the value of $\Delta$ becomes quite independent of $t > t_*$ and $t_0 < t_*$. Therefore, under quite general conditions, we can approximate $\Delta(t)e^{\Psi(t)} \simeq \Theta(t-t^*)\Delta e^{\Psi(t)}$, where $\Theta$ is the Heaviside step function, and

$$\Delta = -i\int_{t_-}^{t_+} dt f(t) e^{-\Psi(t)}. \tag{24}$$

The precise values of $t_-$ and $t_+$ are of little importance in the evaluation of this integral, only that they are far enough from $t_*$ that the integrand is negligible at them. We thus arrive at

$$R(t) \simeq \mathcal{R}^{\text{ad.}}(t) + [A + \Theta(t-t_*)\Delta]\, e^{\Psi(t)}, \tag{25}$$

where $A = [R(t_0) - \mathcal{R}^{\text{ad.}}(t_0)]e^{-\Psi(t_0)}$ depends on the initial condition.

From Eq. (25), and the analogous expression for a segment that follows $R^{\text{n.ad.}}(t)$, we construct our piece-wise addition of segments by determining the exit time $t_+$ of a segment from the condition $|R(t_+)| = 1$, i.e. when the solution is 'half-way between' $R^{\text{ad.}}(t)$ and $R^{\text{n.ad.}}(t)$, and then using this as the entry time $t_-$ for the next segment.

Two effects may cause this transition. Firstly, if the solution does not have enough time to approach, e.g., $R^{\text{ad.}}(t)$ sufficiently closely by the critical time, then the finite difference $|R(t_*) - R^{\text{ad.}}(t_*)|$ will be exponentially amplified after $t = t_*$. This mechanism is responsible, e.g., for the initial transitions one observes in a single encircling of an EP, where the system is initialised to $R(0) = 0 \not\approx R^{\text{ad.}}(t)$. Secondly, however, we see that even for $A = 0$ a destabilisation occurs due to a dynamical mechanism represented by $\Delta \neq 0$, which yields the time of stability loss $t_+$ via

$$|\Delta e^{\Psi(t_+)}| = 1. \tag{26}$$

The time $t_+$ determined in this way is independent of transients and therefore characterises the longest time the solution can remain stable after $t_*$. In the quasi-adiabatic limit $\varepsilon(t) \to 0$ this is not only independent of transients but also of adiabaticity, and is in fact the so-called *maximal delay time* $t_+^*$ (see Appendix A 5 for more details).

### D. Analytic examples

Here we consider three examples analytically in order to illustrate our generalised quasi-adiabatic solution: a circular $\lambda(t)$ as in Sec. III B; a linear $\lambda(t)$ corresponding to the lowest order Taylor expansion; an elliptical $\lambda(t)$ corresponding to the lowest order Fourier expansion. The first example serves to verify that our generalised quasi-adiabatic solution recovers the more specific analytic results in Sec. III B. The second and third examples serve to illustrate the sensitivity of $\Delta$ and therefore $t_+$ in Eq. (26) to the global path—stability loss delay is a global phenomenon. Note that a circular, elliptical, or linear $\lambda(t)$ does not precisely correspond to a circular, elliptical, or linear path in parameter space unless we are in, say, the limit $r \ll 1$. We study particular paths in parameter space numerically in Sec. III E.

*Circular* $\lambda(t)$.—From Sec. III B,

$$\lambda(t) = i\sqrt{r\gamma}e^{-i\pi t/T} \text{ and} \tag{27}$$

$$f(t) = \frac{i\pi}{2T}. \tag{28}$$

The adiabatic fixed point with corrections is

$$\mathcal{R}^{\text{ad.}}(t) = -\varepsilon e^{i\pi t/T} \sum_{n=0}^{N-1} n! \left(2i\varepsilon e^{i\pi t/T}\right)^n \tag{29}$$

where $\varepsilon = \pi/4\sqrt{r\gamma}T$ and the optimal truncation is $N \sim (2\varepsilon)^{-1}$. Furthermore, about $t_* = 3T/2$

$$\Psi(t) = \frac{1}{2\varepsilon}(ie^{-i\pi t/T} + 1) \text{ and} \tag{30}$$

$$\Delta = -\pi e^{-\frac{1}{2\varepsilon}}. \tag{31}$$

Putting these expressions together in Eq. (25) recovers Eq. (16), and solving for $t_+$ in Eq. (26) yields the delay time

$$t_+ - t_* = \frac{T}{\pi}\arccos(2\varepsilon \log \pi), \tag{32}$$

which in the limit $\varepsilon \to 0$ becomes $t_+ - t_* = T/2$, in agreement with Sec. III B.

*Linear* $\lambda(t)$.—Let us now consider another important scenario, where the line of instability is crossed in a linear sweep,

$$\lambda(t) = \lambda_\Re + i\dot{\lambda}_\Im t \text{ and} \tag{33}$$

$$f(t) \simeq f(t_*) = \text{const} \tag{34}$$

where $\dot{\lambda}_\Im > 0$. In this case we have $\Psi(t) = -2i\lambda_\Re t + \dot{\lambda}_\Im t^2$ about $t_* = 0$ and the discontinuity is

$$\Delta = -if(t_*)\sqrt{\frac{\pi}{\dot{\lambda}_\Im}}e^{-\lambda_\Re^2/\dot{\lambda}_\Im}. \tag{35}$$

From these expressions we deduce the delay time

$$t_+ - t_* = \frac{\lambda_\Re}{\dot{\lambda}_\Im}\sqrt{1 + \frac{\dot{\lambda}_\Im}{\lambda_\Re^2}\log\left(\sqrt{\frac{\dot{\lambda}_\Im}{\pi}}\frac{1}{|f(t_*)|}\right)}, \tag{36}$$

which, in the quasi-adiabatic limit becomes $t_+ - t_* = \lambda_\Re/\dot{\lambda}_\Im$. One might naïvely hypothesize that Eq. (35) describe more general paths by using $\lambda_\Re = \Re\lambda(t_*)$ and $\lambda_\Im = \Im\dot{\lambda}(t_*)$. However, a comparison with the circular path above already shows that this would only give rather poor quantitative results. Eq. (36) may still serve for a first estimate of the expected delay times in general scenarios.

*Elliptical* $\lambda(t)$.—As an interpolation between the two cases above we consider the lowest order Fourier expansion of $\lambda(t)$ about $t = t_*$:

$$\lambda(t) = \lambda_\Re \cos(\pi t/T) + i\frac{T\dot{\lambda}_\Im}{\pi}\sin(\pi t/T) \text{ and} \tag{37}$$

$$f(t) \simeq f(t_*) = \text{const}. \tag{38}$$

With $\lambda_\Re = T\dot{\lambda}_\Im/\pi = \sqrt{r\gamma}$ one recovers the circular $\lambda(t)$, and for $T \to \infty$, but keeping $\dot{\lambda}_\Im$ fixed one recovers the linear sweep of $\lambda(t)$. For this example the discontinuity is

$$\Delta = -2iTf(t_*)e^{-\frac{2T^2\dot{\lambda}_\Im}{\pi^2}}I_0\left(\frac{2T}{\pi}\sqrt{\frac{T^2\dot{\lambda}_\Im^2}{\pi^2} - \lambda_\Re^2}\right), \tag{39}$$

where $I_0$ is the first order modified Bessel function of the first kind. By taking the appropriate limits—$I_0(x) \sim 1$ for $x \ll 1$ and $x \in \mathbb{R}^+$ (see, e.g., 9.6.7 in Ref. [48]) for the circular $\lambda(t)$ and $I_0(x) \sim e^x/\sqrt{2\pi x}$ for $x \gg 1$ and $x \in \mathbb{R}^+$ (see, e.g., 9.6.30 and 9.7.1 in Ref. [48]) for the linear $\lambda(t)$—one recovers either Eq. (31) or Eq. (35). Therefore, Eq. (39) interpolates between the two limiting cases above and can be used to accurately calculate delay times for situations where the encircling path lies somewhere in between.

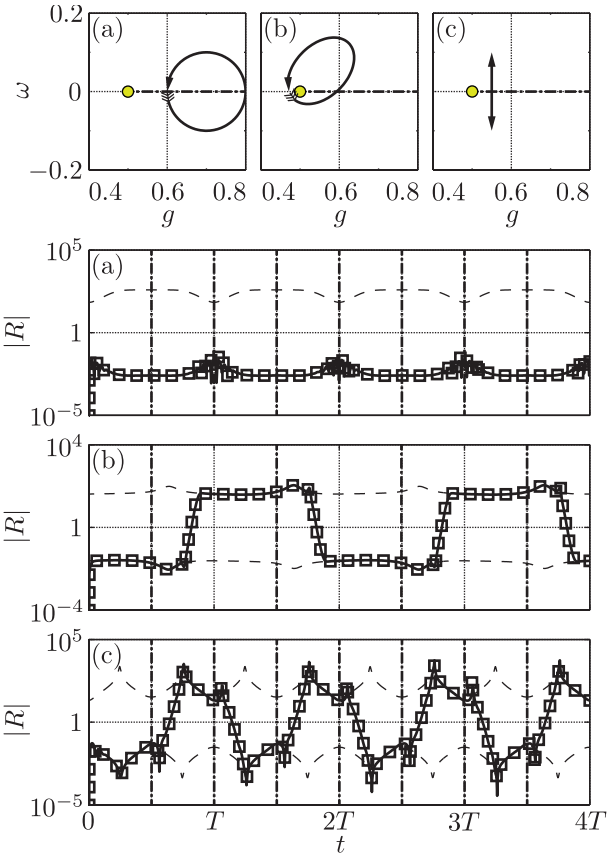


FIG. 4. (Colour online.) Plots of $|R(t)|$ (three bottom panels) for three different paths (top row). In every plot of $|R(t)|$ the solid line is our generalised quasi-adiabatic solution, the open squares denote the numerical solution, the dashed lines denote $\mathcal{R}^{\text{ad.}}(t)$ and $\mathcal{R}^{\text{n.ad.}}(t)$, and the dot-dashed lines denote critical times $t_*$. For the plots of the path, the yellow-filled circle marks the position of the EP and the dot-dashed line is the critical line where $\Im\lambda = 0$. The parameter settings chosen are: (a) $r = 0.1$, $T = 200$, and $g_{\text{o.s.}} = 0.2$; (b) $r = 0.1$, $T = 200$, $e = 0.75$, and $\theta_{\text{aa.}} = \pi/4$; (c) $L = 0.2$, $T = 200$, and $g_{\text{o.s.}} = 0.05$ (see the main text for details on the parametrisation).

### E. Numerical examples

Let us now demonstrate the validity of our approach numerically for more general examples depicted in Fig. 4:

(a) a displaced circular path, $\omega(t) = r\sin\phi(t)$ and $g(t) = \gamma/2 + r\cos\phi(t) + g_{\text{o.s.}}$ where $\phi(t) = 2\pi t/T$ and $g_{\text{o.s.}}$ is a variable off-set in the coupling;

(b) a tilted elliptical path, $\omega(t) = r(t)\sin\phi(t)$ and $g(t) = \gamma/2 + r(t)\cos\phi(t)$ where $\phi(t) = 2\pi t/T$, $r(t) = r_0(1 - e^2)/\{1 + e\cos[\phi(t) + \theta_{\text{aa.}}]\}$, $e$ is the ellipticity and $\theta_{\text{aa.}}$ is the angle of the apoapsis;

(c) oscillations along a straight path which crosses the critical line, $\omega(t) = -L\sin\phi(t)$ and $g(t) = \gamma/2 + g_{\text{o.s.}}$ where $\phi(t) = 2\pi t/T$.

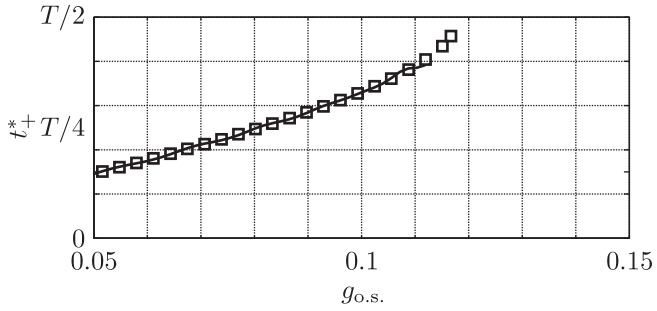


FIG. 5. A plot of the departure time $t_+$ for path (c) in Fig. 4 with the same parametrisation, except for $g_{\text{o.s.}}$, which we vary. The solid line is $t_+$ as determined by Eq. (26) and the open squares denote the numerically observed departure time as determined via $|R(t)| = 1$. Good agreement is exhibited between the analytic $t_+$s and the numerical $t_+$s. A particularly interesting feature is that $t_+$ becomes infinite for $g_{\text{o.s.}} \gtrsim 0.12$. For large $g_{\text{o.s.}}$ one then expects the system to remain adiabatic for all times, as observed in Fig. 4(a).

For these examples the numerically simulated solution $R(t)$ is plotted in Fig. 4 and compared with the generalised quasi-adiabatic solution presented in Sec. III C, with $\Delta$ being evaluated numerically. We see that in all cases the numerical and analytic results match up perfectly.

Let us first consider path (a). For this path there are two dynamical bifurcations in every period, as indicated, but the departure time as determined by Eq. (26) is infinite. Therefore, the solution never has enough time to be significantly repelled from $R^{\text{ad.}}(t)$ before $R^{\text{ad.}}(t)$ becomes stable once again. As a result, the system never leaves the neighbourhood of $R^{\text{ad.}}(t)$, i.e., the solution is adiabatic. In some sense, the increased frequency of dynamical bifurcations and the long departure time has stabilised the adiabatic prediction. In path (b) the opposite is the case. Here the solution undergoes a non-adiabatic transition every period. The solution looks quite similar to that shown in Fig. 4(a), except that the non-adiabatic transitions occur earlier. One finds in this case that the delay time is roughly $0.32T$, slightly less than $T/2$. Finally, in path (c) we have chosen again a path with two dynamical bifurcations per period, but in this case the departure time is roughly $0.15T$, significantly less than $T/2$. Accordingly, we observe two non-adiabatic transitions per period.

The last case can in fact be made to resemble either of the former two cases by tuning $g_{\text{o.s.}}$, i.e., by changing the value of $\lambda_{\Re}(t_*)$. In Fig. 5 we have plotted the departure time as a function of $g_{\text{o.s.}}$. For $g_{\text{o.s.}} < 0.05$ the quasi-adiabatic condition breaks down. For $0.05 < g_{\text{o.s.}} \lesssim 0.12$, i.e., close to the EP, the solution resembles Fig. 4(c) and we observe two non-adiabatic transitions in every period. And around $g_{\text{o.s.}} = 0.12$ the departure time becomes infinite, which implies that for $g_{\text{o.s.}} \gtrsim 0.12$ the dynamics becomes fully adiabatic and resembles Fig. 4(a).

## IV. NOISE

Finally, it is important to address the influence of noise, which will be present in any experimental implementation. To do so we simulated the dynamics of $c_{\mp}$ in the presence of delta-correlated Gaussian noise $\xi(t)$ with variance $\langle \xi(t)\xi(t')\rangle = \gamma N \delta(t-t')$. The gray shaded area in Fig. 3(a) indicates the resulting distribution of stochastic trajectories of $R(t)$ for $N = 1/10$. This resembles the case where the initial resonator amplitude is a factor of 10 above the thermal noise floor. For the first encircling period the fixed point $R^{\text{n.ad.}}(t)$ is still robust, but the delay time $t_+$ is significantly reduced. This again demonstrates the extreme sensitivity of Eq. (11) upon initial conditions. However, the dynamics of $R$ is self-correcting, and after the first encircling period it settles into robust periodic dynamics much resembling the case without noise. This surprising observation can be understood as follows. Initially, noise causes $R$ to loose stability early. But this means that the total population of the system is increased, and therefore the effect of the constant noise background is reduced.

## V. CONCLUSION

In summary, we have analyzed the quasi-adiabatic evolution of non-Hermitian systems near an EP. Our study shows that various dynamical phenomena associated with this process can be predicted from the analysis of the non-adiabatic transition amplitudes, $R_-(t)$ and $R_+(t)$. In particular, we identified a characteristic switching pattern and stability loss delay. Our analytic predictions for the delay times and the observed robustness with respect to noise are relevant for first experimental investigations of these effects and provide the basis for analysing similar phenomena in more complex systems.

*Acknowledgments.* The authors thank M. V. Berry, E.-M. Graefe, M. Koller, D. O. Krimer, A. Mailybaev, A. Neishtadt, and R. Uzdin for useful input. This work was supported by the European FP7/ITC Project SIQS (600645), project OPSOQI (316607) of the WWTF, the Austrian Science Fund (FWF) through SFB FOQUS F40, SFB NextLite F49-10, project GePartWave No. I 1142-N27, and the START grant Y 591-N16.

### Appendix A: Non-standard analysis of relative non-adiabatic transition amplitues

In this appendix we briefly summarise the motivation for the non-standard analysis of quasi-adiabatic non-Hermitian systems [24, 45, 46] and its application to relative non-adiabatic transition amplitudes [34, 49–52]. In order to facilitate a simple but rigorous mathematical treatment we augment the notation of the paper by introducing a dimensionless time

$$s := \frac{t}{T}, \tag{A1}$$

where $T^{-1}$ is considered 'small', and rewrite the governing equation of motion

$$\dot{\mathcal{U}} = -i\mathbf{M}(s)\mathcal{U} \tag{A2}$$

with $\mathcal{U}(0) = 1$ and where $\mathcal{U}$ is the evolution operator and the dot denotes the derivative with respect to time $t$ as usual.

#### 1. Quasi-adiabaticity

We assume $\mathbf{M}(s)$ to be diagonalisable with eigenvalues $\lambda_i(s)$ for all $s$. Since $\mathbf{M}(s)$ is non-Hermitian it does not in general have an orthonormal eigenbasis in the sense of Dirac but rather a biorthogonal eigenbasis: a set of right eigenvectors $\vec{r}_i(s)$ defined via $\mathbf{M}(s)\vec{r}_i(s) = \lambda_i(s)\vec{r}_i(s)$ and a set of left eigenvectors $\vec{l}_i^T(s)$ defined via $\vec{l}_i^T(s)\mathbf{M}(s) = \vec{l}_i^T(s)\mathbf{M}(s)$ such that $\vec{l}_i^T(s)\vec{r}_j(s) = \delta_{i,j}$. Ideal adiabatic dynamics may be defined as that for which the dynamical coefficients of the instantaneous eigenvectors decouple. In a parallel transported eigenbasis, i.e., $\vec{l}_i^T(s)\vec{r}_i'(s) = 0$ where the prime denotes the derivative with respect to $s$, the adiabatic solution, or adiabatic prediction, is

$$\mathcal{U}_{i,j}(t) = \delta_{i,j} \tag{A3}$$

where we have expanded the evolution operator $\mathcal{U}$ thus

$$\mathcal{U}(t) = \sum_{i,j} \mathcal{U}_{i,j} e^{-iT\int_0^s ds'\lambda_i(s')} \vec{r}_i(s)\vec{l}_j^T(0). \tag{A4}$$

In the adiabatic solution the interaction between the dynamical coefficients of the instantaneous eigenvectors due to the finite variation of these eigenvectors is ignored. The full equation of motion for $\mathcal{U}$ expanded as above is

$$\dot{\mathcal{U}}_{p,q} = -i\sum_{i\neq p} T^{-1}\tilde{f}_{p,i}(s) e^{-iT\int_0^s ds'[\lambda_i(s')-\lambda_p(s')]}\mathcal{U}_{i,p} \tag{A5}$$

where we have defined

$$\tilde{f}_{p,i}(s) := -i\vec{l}_p^T(s)\vec{r}_i'(s). \tag{A6}$$

The adiabatic solution ignores $\tilde{f}_{p,q}(s)$ for $p \neq q$. Assuming the system to be initialised to instantaneous eigenvector $q$, first order perturbation theory yields that the solution for the coefficient $x_p$ of instantaneous eigenvector $p$ where $p \neq q$ is

$$x_p(t) \simeq \frac{T^{-1}\tilde{f}_{p,q}(s) e^{-iT\int_0^s ds'[\lambda_q(s')-\lambda_p(s')]}}{\lambda_q(s)-\lambda_p(s)}. \tag{A7}$$

This expression vanishes linearly with $|T^{-1}/[\lambda_q(s) - \lambda_p(s)]$ but diverges exponentially with $T\Im\int_0^s ds'[\lambda_q(s') -$

$\lambda_p(s')]$ if $\int_0^s ds'\lambda_q(s') > \int_0^s ds'\lambda_p(s')$. Second order perturbation theory contains no more information as regards $x_p$ but does reveal that $x_q(t)$ differs from unity with an analogous scaling. The traditional quantum adiabatic condition

$$\varepsilon_{p,q}(t) := \left| \frac{T^{-1}\tilde{f}_{p,q}(s)}{\lambda_q(s) - \lambda_p(s)} \right| \ll 1 \tag{A8}$$

therefore only ensures adiabaticity for those elements of $\mathcal{U}$ for which $\Im \int_0^s ds'\lambda_i(s')$ is greatest, i.e., the least dissipative instantaneous eigenvectors. It obviously cannot be the case that every eigenvector is least dissipative, unless all are degenerate, and it is therefore impossible that the adiabatic solution Eq. (A3) hold. In the context of non-Hermitian systems it therefore seems pertinent to call Eq. (A8) the *quasi*-adiabatic condition. So long as we initialise to the least dissipative instantaneous eigenstate and so long as this eigenstate remains the least dissipative, the quasi-adiabatic condition ensures adiabaticity. But if we initialise to an eigenstate that is not the least dissipative, or the quality of being least dissipative is exchanged, then perturbation theory breaks down.

### 2. Relative non-adiabatic transition amplitudes as a slow-fast system

In the main text we argued that for our two-dimensional case the simplest encompasing dynamical description of adiabaticity is afforded by the relative non-adiabatic transition amplitudes—the ratios of the elements of the evolution operator expressed in a parallel transported eigenbasis. Let us recall the equation of motion for the relative non-adiabatic transition amplitude $R(t)$ as defined in the paper:

$$\dot{R} = -2i\lambda(s)R - iT^{-1}\tilde{f}(s)(1+R^2). \tag{A9}$$

Treating $\lambda$ and $\tilde{f}$ as dynamical variables themselves, in the limit $T^{-1} \to 0$ this becomes

$$\dot{R} = -2i\lambda(s_0)R - iT^{-1}\tilde{f}(s_0)(1+R^2) \tag{A10}$$

where $s_0 = T^{-1}t_0$ and $t_0$ is the initial time. On the other hand, we may rewrite the equation of motion using $s$ as the independent variable,

$$T^{-1}R' = -2i\lambda(s)R - iT^{-1}\tilde{f}(s)(1+R^2), \tag{A11}$$

whereupon similarly taking $T^{-1} \to 0$ yields

$$0 = -2i\lambda(s)R - iT^{-1}\tilde{f}(s)(1+R^2). \tag{A12}$$

The difference between Eqs. (A10) and (A12) is that the former is over a time-scale of order $T^{-1}$ and is hence *fast*, whilst the latter is over a time-scale of order 1 and is hence *slow*; we have a slow-fast system. Furthermore, we notice here that the fast time-scale equation is differential whilst the slow algebraic. This is often taken as the definition of a singularly perturbed system and it means that any perturbative approach in $T^{-1}$ can only be valid for times of order $T^{-1}$. In order to study the long time behaviour we must turn to non-standard analysis.

### 3. Slow manifolds

The solutions of the slow time-scale Eq. (A12) are the fixed points of the fast time-scale Eq. (A10) and as such are known as *instantaneous* fixed points. We recall their approximate expressions from the main text:

$$\begin{aligned} R^{\text{ad.}}(s) &\simeq -\frac{T^{-1}\tilde{f}(s)}{2\lambda(s)} \text{ and} \\ R^{\text{n.ad.}}(s) &\simeq -\frac{2\lambda(s)}{T^{-1}\tilde{f}(s)}. \end{aligned} \tag{A13}$$

Since these are the fixed points of Eq. (A10) we may use Eq. (A10) to perform a stability analysis. One finds that $R^{\text{ad.}}(s)$ is stable if and only if $\Im\lambda(s) < 0$, whilst $R^{\text{n.ad.}}(s)$ is stable if and only if $\Im\lambda(s) > 0$, and the possible local phase portraits are stable star, stable spiral, centre, unstable spiral, and unstable star [53]. Evidently, the only possible bifurcation is from a stable spiral to an unstable spiral through a centre. The locus of points $R^{\text{ad.}}(s)$ over $s$ is called a slow manifold and denoted $M^{\text{ad.}} = \{R^{\text{ad.}}(s) : s\}$. Similarly for $R^{\text{n.ad.}}(s)$.

### 4. Adiabatic manifolds

Due to finite variations in $\lambda(s)$ and $\tilde{f}(s)$ the slow manifolds $M^{\text{ad.}}$ and $M^{\text{n.ad.}}$ are in fact not locally invariant. Nevertheless, a theorem due to N. Fenichel [54] ensures the existence of locally invariant manifolds in a $T^{-1}$-neighbourhood of $M^{\text{ad.}}$ and $M^{\text{n.ad.}}$. These locally invariant manifolds are called adiabatic manifolds and denoted $\mathcal{M}^{\text{ad.}}$ and $\mathcal{M}^{\text{n.ad.}}$ respectively. The adiabatic manifolds do not obey a simple equation of motion, but we may find a good approximation by considering the particular integral of the $N$-times linearised equation of motion. We focus on $\mathcal{M}^{\text{ad.}}$ for clarity. Following the argument of example 2.1.10 in Ref. [34] one arrives at $\mathcal{M}^{\text{ad.}} = \{\mathcal{R}^{\text{ad.}}(s) : s\}$ where

$$\mathcal{R}^{\text{ad.}}(s) \simeq \sum_{n=0}^{N-1} T^{-n} \left( \frac{-1}{2i\lambda(s)} \frac{d}{ds} \right)^n R^{\text{ad.}}(s) \tag{A14}$$

and $N$ is an optimal truncation with a remainder of order $e^{-C/T^{-1}}$ for some $C > 0$. The expression for $\mathcal{R}^{\text{n.ad.}}(s)$ is analogous. We describe $\mathcal{R}^{\text{ad.}}(s)$ and $\mathcal{R}^{\text{n.ad.}}(s)$ as attractive or unattractive analogously to $R^{\text{ad.}}(s)$ and $R^{\text{n.ad.}}(s)$ being stable or unstable respectively.

### 5. Stability loss delay

At certain critical times $t_*$, or $s_*$, the stability of the instantaneous fixed points swaps. For example, $R^{\text{ad.}}(s)$ becomes unstable and $R^{\text{n.ad.}}(s)$ becomes stable at $s = s_*$ such that $\Im\lambda(s_*) = 0$ and $\Im\lambda'(s_*) > 0$. One might naïvely suppose an immediate transition between $M^{\text{ad.}}$ and $M^{\text{n.ad.}}$ at $s = s_*$, but this is not the case. The bifurcation is dynamical and the type is degenerate Hopf, which in general exhibits the phenomenon known as *stability loss delay*: the solution $R(t)$ continues to follow, say, $R^{\text{ad.}}(s)$ for a significant time past its loss of stability. Following the argument in Sec. 2 of Ref. [52] one finds that away from $s = s_*$ the solution has the asymptotic expansion

$$R(t) \sim Ae^{\tilde{\Psi}(s)/T^{-1}} + \mathcal{R}^{\text{ad.}}(s) \tag{A15}$$

where

$$\tilde{\Psi}(s) = -2i\int_{s_*}^{s} ds'\lambda(s'), \tag{A16}$$

whilst at $s = s_*$ the solution exhibits the discontinuity

$$\Delta = -i\int_{s_-^*}^{s_+^*} ds\tilde{f}(s)e^{-\tilde{\Psi}(s)/T^{-1}} \tag{A17}$$

where $s_-^* < s_*$ and $s_+^* > s_*$ are the intersections of the level curve of $\Re\Psi$ that includes the point $z_* \in \mathbb{C}$ such that $\lambda(z_*) = 0$. In order to incorporate this discontinuity in the asymptotic expansion of the solution for $R(t)$ we add the term $\Theta(s - s_*)\Delta e^{\tilde{\Psi}(s)/T^{-1}}$ where $\Theta$ is the Heaviside step function. This term is proportional to $e^{(\tilde{\Psi}(s)-\tilde{\Psi}(z_*))/T^{-1}}$, and therefore diverges as $T^{-1} \to 0$ for any time $t$ such that $\Re\tilde{\Psi}(s) - \Re\tilde{\Psi}(z_*) > 0$. Thus, the times $t_-^* < t_*$ and $t_+^* > t_*$ corresponding to $s_-^*$ and $s_+^*$ are such that:

(i) if the solution enter a neighbourhood of $M^{\text{ad.}}$ before $t_-^*$ then it must leave at $t_+^*$;

(ii) if the solution enter a neighbourhood of $M^{\text{ad.}}$ after $t_-^*$ at $t_- < t_*$ then it must leave at $t_+ > t_*$ such that $\Re\tilde{\Psi}(s_+) - \Re\tilde{\Psi}(s_-) = 0$;

(iii) if the solution leave a neighbourhood of $M^{\text{ad.}}$ after $t_+^*$ then it must have entered at $t_-^*$.

Since the third case is sure to be rare, one typically calls $t_+^*$ the *maximal delay time*. Note that, this maximal delay time is precisely the quasi-adiabatic limit of the delay time $t_+$ calculated via Eq. (26).

For an analytic example of a maximal delay time, let us consider the path analysed in Sec. III B. In this case the level curves of $\Re\tilde{\Psi}$ are

$$e^{-\pi\Im z}\cos(\pi\Re z) \simeq \text{const.} \tag{A18}$$

Evidently, any $s_- < 0$ such that $s_- > -1/2$ is connected to $s_+ = -s_- > 0$ by these level curves. The maximal delay time is therefore $t_+^* = T/2$, which agrees with the main text.

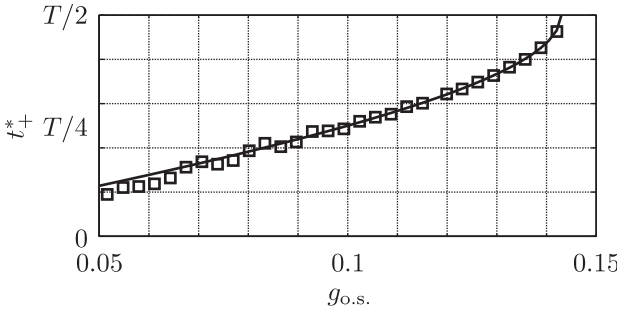


FIG. 6. Plot of the theoretical maximal delay time (solid line) and numerically observed departure times from a 5%-neighbourhood of $R^{\text{ad.}}(s)$ (open squares) for case (c) from Sec. III E.

For a numerical example, let us consider case (c) from Sec. III E. Here we calculate the theoretical maximal delay time by numerically finding the complex root of $\lambda(z)$, i.e., $z_*$, and then numerically finding where the level curve of $\Re\tilde{\Psi}$ on which $z_*$ lies intersects the real axis. The results are plotted in Fig. 6. Also plotted in the figure are the results of a numerical solution where we have initialised to a neighbourhood of $R^{\text{ad.}}(s)$ at $s = s_-^*$ and asked for when the numerical solution departs from this neighbourhood. The agreement between the theoretical maximal delay time and the numerically observed departure time is very good. Furthermore, we see qualitatively the same results as those shown in Fig. 5; the quantitative difference is simply due to the finite time required for $R(t)$ to leave a small neighbourhood of $M^{\text{ad.}}$ and reach $|R(t)| = 1$.

## Appendix B: Non-adiabatic transitions as a manifestation of the Stokes phenomenon of asymptotics

The Stokes phenomenon of asymptotics is that subdominant exponentials in the asymptotic expansion of certain functions disappear and reappear in different sections of the complex plane with different coefficients. In Stokes' words [55],

> ... the inferior term enters as it were into the mist, is hidden for a little while from view, and comes out with its coefficient changed.

M. V. Berry and R. Uzdin [27] uncovered the presence of the Stokes phenomenon of asymptotics in the solutions of specific exactly solvable models of quasi-adiabatic non-Hermitian systems and identify non-adiabatic transitions in such systems as a manifestation. In this appendix we review one such example.

Let us consider again the parametrisation studied in Sec. III B: $\omega(t) = r\sin\phi(t)$, $\gamma(t) = 1$, and $g(t) = 1/2 +$

$r\cos\phi(t)$ with $r \ll 1$ and $\dot{\phi}(t) = \dot{\phi} = 2\pi/T = \text{const}$. An exact solution for this example is presented by M. V. Berry [32] which we now review. Constructing the analagous quantity to $R$ in the circular basis

$$\vec{r}_{\circlearrowleft} = \frac{1}{\sqrt{2}}\begin{pmatrix}1\\ i\end{pmatrix} \text{ and } \vec{r}_{\circlearrowright} = \frac{1}{\sqrt{2}}\begin{pmatrix}1\\ -i\end{pmatrix}, \tag{B1}$$

which we denote $p$, i.e., $\vec{x}(t) = c_{\circlearrowleft}(t)\vec{r}_{\circlearrowleft} + c_{\circlearrowright}(t)\vec{r}_{\circlearrowright}$ and $p(t) = c_{\circlearrowleft}(t)/c_{\circlearrowright}(t)$, one arrives at the equation of motion

$$\dot{p} \simeq re^{i\phi(t)} + p^2, \tag{B2}$$

where we have used $r \ll 1$. Note that, $\vec{r}_{\circlearrowleft}$ and $\vec{r}_{\circlearrowright}$ are not eigenvectors. Introducing the new independent variable $\zeta = (i/2)(2\varepsilon)^{-1}e^{i\phi(t)/2}$ where $\varepsilon = \pi/(4\sqrt{r}T)$ and using the ansatz $p(t) = -(d/dt)\log f(\zeta)$ yields

$$\zeta^2\frac{d^2f}{d\zeta^2} + \zeta\frac{df}{d\zeta} + \zeta^2 f = 0. \tag{B3}$$

This is the zeroth order Bessel equation and the solution from time $t = t_0$ is thus

$$p(t) = \frac{i}{2}\dot{\phi}\zeta\frac{\mathcal{C}_1(\zeta)}{\mathcal{C}_0(\zeta)} \tag{B4}$$

where $\mathcal{C}_n(\zeta) = c_J J_n(\zeta) + c_Y Y_n(\zeta)$ is a linear combination of order $n$ Bessel functions of the first and second kind with the ratio

$$\frac{c_Y}{c_J} = -\frac{2ip(t_0)J_0(\zeta_0) + \dot{\phi}\zeta_0 J_1(\zeta_0)}{2ip(t_0)Y_0(\zeta_0) + \dot{\phi}\zeta_0 Y_1(\zeta_0)} \tag{B5}$$

where $p(t_0)$ is the initial condition for $p$ and $\zeta_0 = (i/2)(2\varepsilon)^{-1}e^{i\phi(t_0)/2}$.

In order to translate this result into an expression for $R(t)$ we have only to transform from the circular basis Eq. (B1) to the original basis and then from that to the parallel transported eigenbasis Eq. (5),

$$\vec{r}_-(t) = \begin{pmatrix}\cos\vartheta(t)/2\\ \sin\vartheta(t)/2\end{pmatrix} \text{ and } \vec{r}_+(t) = \begin{pmatrix}-\sin\vartheta(t)/2\\ \cos\vartheta(t)/2\end{pmatrix} \tag{B6}$$

where $\tan\vartheta(t) = -g(t)/[\omega(t) + i\gamma(t)/2]$. Recognising the effect of such transformations on $p$ and $R$ as Möbius transformations, it is immediately seen that

$$p(t_0) = e^{i\vartheta(t_0)}\frac{1 + iR(t_0)}{1 - iR(t_0)}, \tag{B7}$$

where $R(t_0)$ is the initial condition for $R$, and

$$R(t) = i\frac{1 - e^{-i\vartheta(t)}p(t)}{1 + e^{-i\vartheta(t)}p(t)}. \tag{B8}$$

Let us focus on the asymptotic expansion about $t = t_*$ where $R^{\text{ad.}}(t)$ becomes unstable. Recalling that $\lambda(t) \simeq \sqrt{r}e^{i\phi(t)/2}$ and $\Im\lambda(t_*) = 0$ we see that with $\zeta_* = (i/2)(2\varepsilon)^{-1}e^{i\phi(t_*)/2}$ we have $\Re\zeta_* = 0$. Without loss of generality, we suppose $\Im\zeta_* > 0$. Using 9.1.35, 9.1.36, 9.2.1, and 9.2.2 in Ref. [48] and assuming that the solution is exponentially close to $R^{\text{ad.}}(t)$ by $t = t_*$ yields

$$R(t) \sim i\frac{1 - e^{\vartheta(t)}p^{\text{ad.}}(t) + 2i\Theta(-\Re\zeta)e^{2i\zeta}[1 - e^{\vartheta(t)}p^{\text{n.ad.}}(t)]}{1 + e^{\vartheta(t)}p^{\text{ad.}}(t) + 2i\Theta(-\Re\zeta)e^{2i\zeta}[1 + e^{\vartheta(t)}p^{\text{n.ad.}}(t)]} \tag{B9}$$

for $-\pi/2 < \arg\zeta < 3\pi/2$ where $p^{\text{ad.}}(t)$ and $p^{\text{n.ad.}}(t)$ correspond to $R^{\text{ad.}}(t)$ and $R^{\text{n.ad.}}(t)$ respectively and $\Theta$ is the Heaviside step function. The discontinuity in this asymptotic expansion is precisely the Stokes phenomenon of asymptotics. For $t \in (t_* - T/2, t_* + T/2)$ the discontinuous term is subdominant and $R(t) \sim R^{\text{ad.}}(t)$, whereas for $t > t_* + T/2$ it is dominant and $R(t) \sim R^{\text{n.ad.}}(t)$. The connection to the expansion Eq. (16) from Sec. III B is more clearly seen by expanding to first order about $R^{\text{ad.}}(t)$:

$$R(t) \approx R^{\text{ad.}}(t) - 2\Theta(t - t_*)e^{-\exp(i\phi(t)/2)/(2\varepsilon)}. \tag{B10}$$

Comparing this expansion to Eq. (16) we find very good agreement. The small difference that here the discontinuity at $t = t_*$ is $\Delta = -2e^{-1/(2\varepsilon)}$ whereas in Sec. III D we found $\Delta = -\pi e^{-1/(2\varepsilon)}$ is principally due to the asymptotic expansions employed in calculating Eq. (B9), which differ from those used in calculating Eq. (16).


[1] M. Born, Z. Phys. A-Hadron Nucl. **40**, 167 (1927).

[2] S. G. Johnson, P. Bienstman, M. A. Skorobogatiy, M. Ibanescu, E. Lidorikis, and J. D. Joannopoulos, Phys. Rev. E **66**, 066608 (2002).

[3] E. Farhi, J. Goldstone, S. Gutmann, J. Lapan, A. Lundgren, and D. Preda, Science **292**, 472 (2001).

[4] T. Kato, *Perturbation Theory for Linear Operators* (Springer-Verlag, Berlin, 1995), 2nd ed.
[5] A. P. Seyranian and A. A. Mailybaev, *Multiparameter Stability Theory with Mechanical Applications* (Worl Scientific Publishing, Singapore, 2003).
[6] M. V. Berry, Czech. J. Phys. **54**, 1039 (2004).
[7] A. P. Seyranian, O. N. Kirillov, and A. A. Mailybaev, J. Phys. A: Math. Gen. **38**, 1723 (2005).
[8] I. Rotter, J. Phys. A: Math. Theor. **45**, 153001 (2009).
[9] N. Moiseyev, *Non-Hermitian Quantum Mechanics* (Cambridge Univerity Press, Cambridge, 2011).
[10] W. D. Heiss, J. Phys. A: Math. Theor. **45**, 444016 (2012).
[11] D. C. Brody and E.-M. Graefe, Phys. Rev. Lett. **109**, 230405 (2012).
[12] N. Bachelard, C. Garay, J. Arlandis, R. Touzani, and P. Sebbah, arXiv:1407.8220.
[13] B. Peng, Ş. K. Özdemir, S. Rotter, H. Yilmaz, M. Liertzer, F. Monifi, C. M. Bender, F. Nori, and L. Yang, Science **346**, 328 (2014).
[14] P. Ambichl, K. G. Makris, L. Ge, Y. Chong, A. D. Stone, and S. Rotter, Phys. Rev. X **3**, 041030 (2013).
[15] S. Klaiman, U. Günther, and N. Moiseyev, Phys. Rev. Lett. **101**, 080402 (2008).
[16] C. E. Rüter, K. G. Makris, R. El-Ganeiny, D. N. Christodoulides, M. Segev, and D. Kip, Nat. Phys. **6**, 192 (2010).
[17] M. Brandstetter, M. Liertzer, C. Deutsch, P. Klang, J. Schöberl, H. E. Türeci, G. Strasser, K. Unterrainer, and S. Rotter, Nat. Comm. **5**, 4034 (2014).
[18] C. Dembowski, H.-D. Gräf, H. L. Harney, A. Heine, W. D. Heiss, H. Rehfeld, and A. Richter, Phys. Rev. Lett. **86**, 787 (2001).
[19] T. Gao, E. Estrecho, K. Y. Bliokh, T. C. H. Liew, M. D. Fraser, S. Brodbeck, M. Kamp, C. Schneider, S. Höfling, Y. Yamamoto, F. Nori, Y. S. Kivshar, A. Truscott, R. Dall, and E. A. Ostrovskaya, arXiv:1504.00978.
[20] O. Latinne, N. J. Kylstra, M. Dörr, J. Purvis, M. Terao-Dunseath, C. J. Joachain, P. G. Burke, and C. J. Noble, Phys. Rev. Lett. **74**, 46 (1995).
[21] R. Lefebvre, O. Atabek, M. Šindelka, and N. Moiseyev, Phys. Rev. Lett **103**, 123003 (2009).
[22] O. Atabek, R. Lefebvre, M. Lepers, A. Jaouadi, O. Dulieu, and V. Kokoouline, Phys. Rev. Lett. **106**, 173002 (2011).
[23] A. Kvitsinsky and S. Putterman, J. Math. Phys. **32**, 1403 (1991).
[24] G. Nenciu and G. Rasche, J. Phys. A: Math. Gen. **25**, 5741 (1992).
[25] G. Dridi, S. Guérin, H. R. Jauslin, D. Viennot, and G. Jolicard, Phys. Rev. A **82**, 022109 (2010).
[26] R. Uzdin, A. Mailybaev, and N. Moiseyev, J. Phys. A: Math. Theor. **44**, 435302 (2011).
[27] M. V. Berry and R. Uzdin, J. Phys. A: Math. Theor. **44**, 435303 (2011).
[28] I. Gilary, A. A. Mailybaev, and N. Moiseyev, Phys. Rev. A **88**, 010102 (2013).
[29] A. Leclerc, G. Jolicard, and J. P. Killingbeck, J. Phys. B: At. Mol. Opt. **46**, 145503 (2013).
[30] E.-M. Graefe, A. A. Mailybaev, and N. Moiseyev, Phys. Rev. A **88** 033842 (2013).
[31] D. Viennot, J. Phys. A: Math. Theor. **47**, 065302 (2014).
[32] M. V. Berry, J. Opt. **13**, 115701 (2011).
[33] M. V. Berry, Proc. R. Soc. Lond. A **422**, 7 (1989).
[34] N. Berglund and B. Gentz, *Noise-induced phenomena in slow-fast dynamical systems: a sample-paths approach* (Springer-Verlag, London, 2006).
[35] M. Diener, Math. Intell. **6**, 38 (1984).
[36] A. I. Neishtadt, Discrete Cont. Dyn.-S **35**, 897 (2009).
[37] T. Faust, J. Rieger, M. J. Seitner, J. P. Kotthaus, and E. M. Weig, Nat. Phys. **9**, 485 (2013).
[38] H. Okamoto, A. Gourgout, C.-Y. Chang, K. Onomitsu, I. Mahboob, E. Y. Chang, and H. Yamaguchi, Nat. Phys. **9**, 480 (2013).
[39] X.-W. Xu, Y. Liu, C.-P. Sun, and Y. Li, arXiv:1402.7222.
[40] A. B. Shkarin, N. E. Flowers-Jacobs, S. W. Hoch, A. D. Kashkanova, C. Deutsch, J. Reichel, and J. G. E. Harris, Phys. Rev. Lett. **112**, 013602 (2014).
[41] H. Jing, S. K. Özdemir, X.-Y. Lü, J. Zhang, L. Yang, and F. Nori, Phys. Rev. Lett. **113**, 053604 (2014).
[42] R. Uzdin and M. Moiseyev, Phys. Rev. A **85**, 031804 (2012).
[43] J. Doppler *et al.*, (to be published).
[44] With the choice Eq. (5) for the instantaneous eigenvectors there is no geometric phase [45, 46].
[45] A. Leclerc, D. Viennot, and G. Jolicard, J. Phys. A: Math. Theor. **45**, 415201 (2012).
[46] S. Ibáñez and J. G. Muga, Phys. Rev. A **89**, 033403 (2014).
[47] I. S. Gradshteyn and I. M. Ryzhik, *Table of Integrals, Series, and Products*, A. Jeffrey, and D. Zwillinger (Elsevier, London, 2007), 7th ed.
[48] M. Abramowitz and I. A. Stegun, *Handbook of Mathematical Functions With Formulas, Graphs, and Mathematical Tables*, tenth printing (Dover, New York, 1972).
[49] A. Bohun, MSc Thesis, Imperial College, London (2011).
[50] A. I. Neishtadt, Diff. Equat. **23**, 1385 (1987).
[51] A. I. Neishtadt, Diff. Equat. **24**, 171 (1988).
[52] F. Diener and M. Diener, "Maximal Delay", *Dynamical Bifurcations* (Springer, Berlin, 1991).
[53] P. Glendinning, *Stability, Instability and Chaos: an Introduction to the Theory of Nonlinear Differential Equations* (Cambridge University Press, 1994).
[54] N. Fenichel, J. Differ. Equations **31**, 53 (1979).
[55] G. G. Stokes, Acta Math. **26**, 393 (1902).